Journal of Ceramic Processing Research. Vol. 17, No. 3, pp. 240~245 (2016)

J O U R N A L O F
Ceramic
Processing Research

Fabrication and property evaluation of Al-1 wt.%Si-0.5 wt.%Cu sputtering target materials by spark plasma sintering Process

Ik-Hyun Oh[a,*], Jun-Ho Jang[a,d], Jun-Mo Yang[c], In-Jin Shon[b], Jae-Won Lim[d] and Hyun-Kuk Park[a,b,*]

[a]*Korea Institute of Industrial Technology (KITECH), Automotive Components Group, 1110-9 Oryong-dong, buk-gu, Gwang-Ju 500-480, Korea*

[b]*Division of Advanced Materials Engineering and Research Center of Advanced Materials Development, Chonbuk National University, 664-14 Deokjin-dong 1-ga, Deokjin-gu, Jeonju, Jeonbuk 561-756, Korea*

[c]*Measurement & Analysis Team, National Nanofab Center, Daejeon 305-806, Korea*

[d]*Division of Advanced Materials Engineering, Chonbuk National University, 664-14 Deokjin-dong 1-ga, Deokjin-gu, Jeonju, Jeonbuk 561-756, Korea*

Al-Si-Cu alloy targets were fabricated using the spark plasma sintering (SPS) process for sputtering target applications. Powder for sintering of the Al-Si-Cu alloy compacts was prepared using the gas atomizing process. For fabricating the Al-Si-Cu alloy compacts, optimized sintering conditions such as temperature, pulse ratio, pressure, and heating rate were controlled during the sintering process. Al-Si-Cu alloy sputtering target materials after sintering using gas atomized powder were 200 mm in diameter and 6.35 mm in thickness. In addition, the SPSed sputtering targets and thin films were compared with those of a commercial target fabricated using the casting melting process. The sputtering targets materials having a relative density of 100% were fabricated under the uniaxial pressure range of 40 ~ 60 MPa at a sintering temperature of 400 °C. Grain size of the SPSed target materials decreased with increasing of sintering pressure at the same temperature of 400 °C. Also, the purity of the SPSed target materials was 99.992%. The properties of thin films deposited on a Si substrate using the SPSed target materials were compared with those of the commercial target material prepared using the casting melting process. From the results, the specific resistivity of thin film deposited using the SPSed target material was 4.4 μΩm, which was a similar value (4.5 μΩm) to that of the commercial thin film.

Key words: Al-Si-Cu sputtering target, Spark plasma sintering, Thin film, Device interconnection lines.

Introduction

Al and Al alloys are widely used as interconnecting materials in microelectronic devices [1-5]. The most commonly used alloying elements in Al interconnect lines are Si and Cu. Si is added in concentrations up to 1 wt.% to minimize the non-uniform interdiffusion of Si into Al in the contact region, known as “spiking”. Cu is added, usually between 0.5 and 4 wt.%, to reduce the electromigration failure rate. To overcome these problems, Al-Si-Cu alloys have recently been used as the sputtering target material for interconnecting lines in Si ICs and electro-mechanical microsystems [6-10]. The Al-Si-Cu sputtering targets are produced either by powder metallurgy or by melting processes for microelectronics device applications. Failures of the interconnection lines, which severely limit the reliability of these devices, can be caused by the insufficient mechanical strength of the materials involved. A fine-grained microstructure is obtained from the powder metallurgical process, which improves the mechanical properties of the final products considerably. Sputtering target materials basically require high density, high purity, low specific resistance, and fine grain size. The characteristics of thin film deposited using the sputtering target materials are determined from the properties of the sputtering target material. Recently, Spark Plasma Sintering (SPS) has been studied and applied to the development of target materials. In this current study, the Al-Si-Cu alloy sputtering target materials were fabricated using the SPS process, which combines a DC pulse current with the application of a high pressure sintering process [6, 11]. This SPS process could operate at a low temperature and for a short time because the powder surface is activated by a high voltage pulse current between gaps in the powder [7, 11]. The key advantages of the SPS process are that it can fabricate a sintered body having high density with a short sintering time and has a fine grain size and high purity [12-14]. Therefore, sputtering target materials fabricated using SPS have good properties compared to those fabricated using the conventional sintering process such as hot press (HP), hot isostatic pressure (HIP), and heat treatment after cold isostatic pressure (CIP). In this study, properties of thin films deposited using the Al-1 wt%Si-0.5 wt.%Cu target

*Corresponding author:
Tel : +82-62-600-6180
Fax: +82-62-600-6149
E-mail: hk-park@kitech.re.kr

fabricated using SPS were compared with those of a commercial target material (TASCO Co., USA) prepared using the casting melting process. For comparison of the properties of both thin films, these target materials were deposited using the same sputtering process on a Si substrate.

Experimental Procedure

In this study, Al (irregular type, 99.999% in purity), Si (irregular type, 99.999% in purity), and Cu (disk type, 99.999% in purity) ingots were used as raw materials for gas atomization. These raw materials were melted under Ar in a graphite crucible. The operation was started by running the atomizing gas into the nozzle, which caused the liquid metal to be drawn up to the tip of the metal flow tube where it was atomized. The vacuum level and gas pressure of the chamber during the process were 6 Pa and 15 atm, respectively, while the orifis diameter was 4 mm and the melting temperature was 1000 °C. The element composition of the raw materials to fabricate the Al-Si-Cu alloy sputter target was Al-1 wt.%Si-0.5 wt.%Cu. After gas atomization, the sizes of the Al-Si-Cu powder were mainly distributed in the range of 55~250 μm and under 38 μm. The obtained powder was sieved in order to use similar sizes of powder in the range of 38 ~ 100 μm for sintering and was sieved in order to sinter similar sizes of powder under 38 μm with a mean diameter of about 12 μm. Fig. 1 shows a schematic diagram of the apparatus used for the SPS process, which includes a 12 V, 30,000 A DC pulse current (which provides a pulsed current with 12 ms on time and 2 ms off time through the target material and through the dies). Unlike conventional powder sintering methods such as HP and HIP, the mechanism of the SPS process involves the DC pulse current flowing directly through the loaded powder in the graphite mold. To fabricate the target materials, the gas atomized powder was filled between two graphite punches in a graphite mold of 200 mm diameter. BN lubricant was sprayed on the graphite punches and inner wall of the mold to avoid the reaction between graphite and Al-Si-Cu powder during sintering. To obtain uniform compaction of the powder, the filled powder was pre-pressured at 50 MPa for 15 min before sintering. Some of the Al-Si-Cu powder was then sintered in a vacuum of 6 Pa and held for 5 min by a uniaxial punch pressure of 60 MPa at a temperature of 400 °C. The heating rate was 60 °C /min in the sintering treatment. The microstructure and composition uniformity of the raw materials, the gas atomized Al-Si-Cu powder, and the SPSed target materials were observed using a scanning electron microscope (SEM) and SEM-EDAX. Also, the purities of these samples were investigated using induction couple plasma (ICP). The relative densities of sintered target materials were calculated based on the theoretical density of 2.704 g/cm^3 using the Archimedes method. Also, grain sizes were measured using the line intercept method. Initially, abnormal grains were identified based on their larger size and orientation angles at the boundaries, and the average grain size was measured by drawing lines in those areas where abnormal grains were absent and at least 40 normal grains were present. X-ray diffraction (XRD) was recorded using Cu-Kα radiation to observe the phase change of the target materials. The fabricated target materials were polished to make a thin film by forming the materials on a grinding machine. The polished surface of the Al-Si-Cu target material was installed in the in-line sputtering system (SRN-120), and the Al-Si-Cu thin film was fabricated for 1 hr at a mixed condition of high pressure and low pressure. In general, this mixed condition is used to obtain outstanding adhesion at the interface between the thin film and the substrate and between substrate and the conductivity of the thin film. The conditions of high pressure (HP) and low pressure (LP) were 3.33 and 0.33 Pa with Ar gas, respectively. Also, Si was used as a substrate. Specific resistivity, depth profiles, microstructures, and the crystallite size of the thin films were measured.

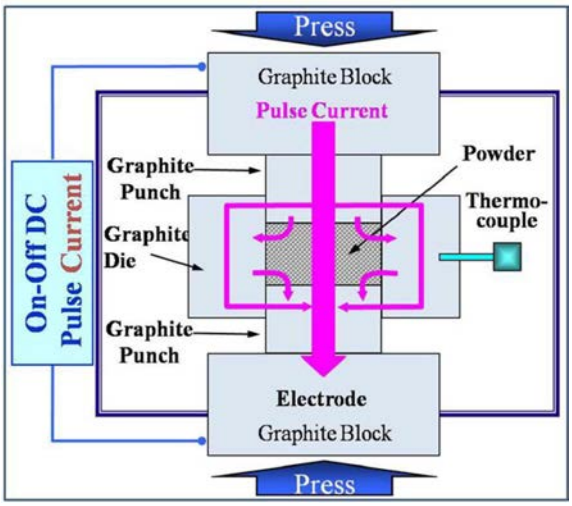

Fig. 1. Schematic diagram of apparatus for spark plasma sintering process.

Result and Discussion

Fig. 2 shows the FE-SEM images of gas atomized Al-1 wt.%Si-0.5 wt.%Cu powder. The particles are almost spherical in shape and have small adhering satellites. The surfaces are slightly irregular and rough, which will induce operating variables involving gas type, alloy type, gas pressure, gas feed rate and velocity, and nozzle geometry [15]. From the SEM-EDAX result, the composition of the gas atomized Al-Si-Cu alloy powder was 98.5 wt.%Al-1.09 wt.%Si-0.41 wt.%Cu, which is

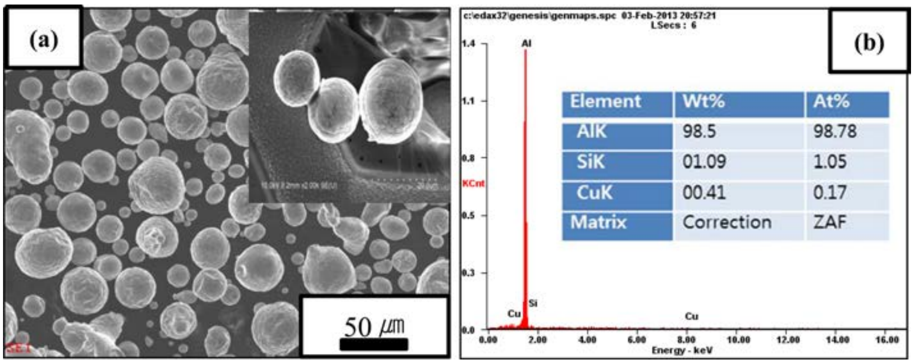

Fig. 2. FE-SEM image and SEM-EDAX for gas atomized Al-Si-Cu powder.

Table 1. Results of Induction Couple Plasma(ICP) analysis for raw material ingot, gas atomized powder and SPSed target materials.

(unit: ppm)

Al-Si-Cu		Al	Cu	Si	Cr	Ca	Mo	Fe	B	P	Mn	Purity
Raw Material ingot	Al	Bal.	1.4	0.6	< 0.5	–	–	2.1	< 0.5	–	–	5N
	Cu	–	Bal.	< 0.5	–	–	–	< 0.5	< 0.5	< 0.5	–	5N
	Si	–	–	Bal.	< 0.5	< 0.5	< 0.5	< 0.5	< 1	–	–	5N
Gas atomized Powder		985,167	5020	10439	8.1	12.4	15.7	11.5	6.6	9.5	18.6	4N1
SPSed target		985,016	4849	10241	5.7	10.5	13.2	8.9	6.7	9.8	15.7	4N2

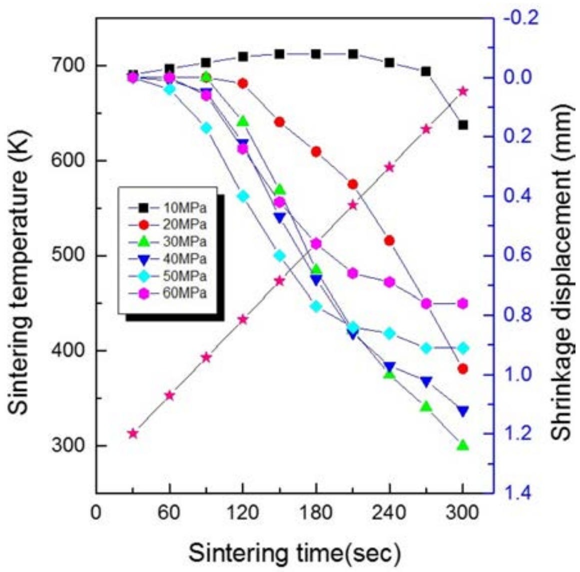

Fig. 3. Variation of Shrinkage displacement with sintering temperature, sintering time and pressure of SPSed target materials.

almost the same as the initial raw material (Al-1.0 wt.%Si-0.5 wt.%Cu) before gas atomization.

Table 1 provides compositions of each element for the raw material ingot, gas atomized powder, and SPSed target material analyzed using induction couple plasma (ICP). In the case of the all raw material ingots for gas atomization, it was found that the purity was 99.999%, which is almost the same as that (99.991%) of the gas atomized alloy powder and SPSed target material. After gas atomization and SPS process, the impurity values of each element were slightly changed and new impurity components were either generated or disappeared such as Mo and P based on the raw material ingots, which could be attributed to the remaining undesirable elements in the chamber and the changing physical properties of elements due to the atomization process. The Oxygen and Nitride gas impurities of SPSed target were 0.029% and < 0.005%, respectively.

The variations of shrinkage displacement of the Al-1 wt.%Si-0.5 wt.%Cu target material with sintering temperature, sintering time, and pressure during the SPS process are shown in Fig. 3. The final sintering temperatures required to fabricate target materials having high density and heating rate up to final temperature were 400 °C and 60 °C/min, respectively. The heating directly progressed up to 400 °C without any holding time. The shrinkage displacement considerably increased with increasing sintering pressure at the same sintering temperature. The beginning temperature of the shrinkage displacement of target materials sintered using the applied pressure range of 20 ~ 60 MPa was about 70 °C. Thereafter, the shrinkage of target materials abruptly increased from about 90 °C. The target material sintered at 10 MPa was linearly progressed with the expansion of volume up to about 210 °C, and thereafter, the shrinkage smoothly progressed up to room temperature. Using the shrinkage displacements data and initial height of powder compact, the height variation of the powder compact ΔL was precisely measured ($\Delta L = L_T - L_0 < 0$, where L_T is the instantaneous height and L_0 is the initial height of the powder compact). The instantaneous relative density D can thus be computed [16]

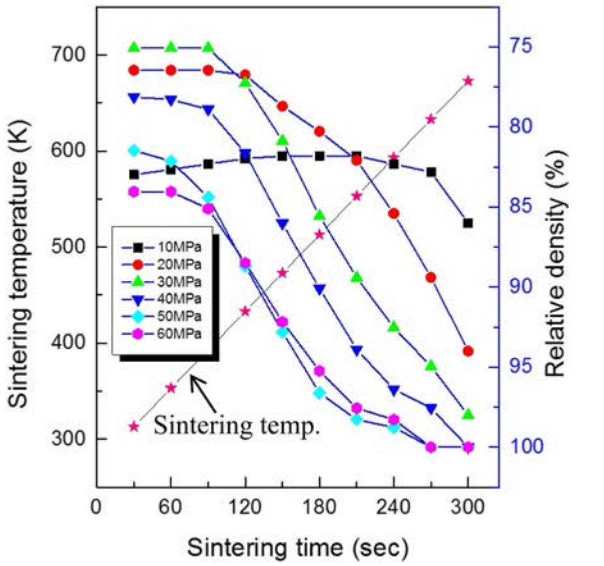

Fig. 4. Variation of relative density with sintering temperature, sintering time and pressure of SPSed target materials.

$$D_T = (L_f / L_T)D_f \quad (1)$$

where D_T is the instantaneous relative density, L_f is the final height, L_T is the instantaneous height, and D_f is the final relative density. Fig. 4 shows that the target material having full relative density of 100% could be obtained at sintering conditions under a pressure range of 40 ~ 60 MPa. However, although the relative densities of these targets are the same as 100% under pressure ranges of 40 ~ 60 MPa, the sintering temperature and the time taken to fabricate target materials having full density considerably differ at each sintering pressure. Consequently, the suitable sintering temperature and pressure are dominant factors governing the high densification behavior of target materials. It should be noted that the present target materials having full density (40 ~ 60 MPa at 400 °C) within 5 min in sintering time since the beginning of heating are promising for sputtering target applications. These results are attributed to two reasons. First, because high joule heating occurs at the point of contact between particles due to an induced current, the spread of atoms is accelerated. In addition, it is considered to be easier to perform sintering at a low temperature because the spread of atoms is accelerated in an electric field. Second, when pressure is applied during sintering, the driving force of the sintering is increased; eq. (2) shows the increased driving force, F_D [11],

$$F_D = \lambda + (P_a r / \pi) \quad (2)$$

where γ is the interfacial energy, and Pa and r are the applied pressure and radius of particle, respectively. Consequently, these results suggest that the most obvious advantages of the SPS process compared with conventional sintering processes are faster heating rates, shorter processing times, and relatively lower temperatures during sintering, allowing for the limitation of grain growth and clean grain boundaries [11, 15].

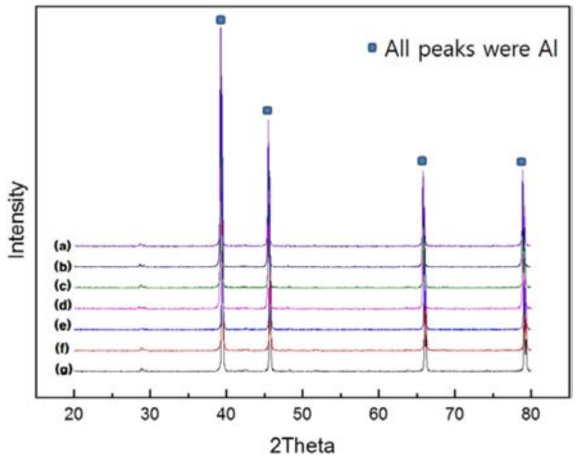

Fig. 5. XRD patterns of the gas atomized powder and the SPSed target material fabricated under pressure range of 10 ~ 60 MPa at 400 °C. (a) gas atomized powder, (b) 10 MPa, (c) 20 MPa, (d) 30 MPa, (e) 40 MPa (f) 50 MPa, (g) 60 MPa.

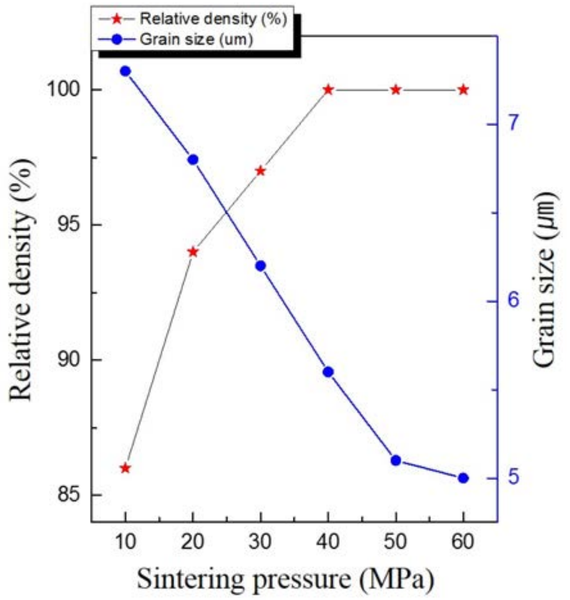

Fig. 6. Relative density and grain size of SPSed target materials fabricated under pressure range of 10 ~ 60 MPa at 400 °C.

Fig. 5 shows the XRD patterns of the gas atomized powder and the SPSed target materials fabricated in the range of 10 ~ 60 MPa at 400 °C. These XRD results demonstrate that the powder and target consist of the typical Al phase, and the added elements of Si and Cu were not observed. This indicates that almost all of the Si and Cu exist as a solid solution with Al. However, in the XRD, a peak was not detected, probably because part of the Si was segregated in the Al alloy because more Si was added than could be soluble in Al.

The relative density and grain size of the SPSed target materials fabricated under a pressure range of

Table 2. Comparison of specific resistivity of commercial and SPSed Al-1 wt.% Si-0.5 wt.% Cu thin film.

Scan size (5 μm)-HP + LP μm	Commercial film	SPSed film
Specific resistivity [μΩm]	4.52	4.41

10 ~ 60 MPa at 400 ºC are shown in Fig. 6. The full densities of 100% were continuously maintained from the applied pressure of 40 MPa at 400 ºC, as mentioned above. Also, the grain size decrease due to the increase in sintering pressure would be associated with the fast densification of powders during sintering. Although the grain size of as-gas atomized powder used in the present work was about 4.1 μm after sintering, it was found that the growth of grain size did not significantly occur after sintering.

Table 2 shows the resistivity values of commercial and SPSed Al-1 wt.%Si-0.5 wt.% Cu thin film deposited on a Si substrate. According to the detail process conditions, Ar gas was first applied at an initial pressure of 6.5×10^{-4} Pa. When the thin film was formed, the pressure was progressed under mixed condition of high pressure (3.33 Pa) and low pressure (0.33 Pa) for 1 hr at room temperature. The scan size of the surface for thin films was 5 μm and specific resistivity was calculated from eq. (3) using the face resistance obtained by a 4 point probe.

$$\rho = L \cdot R/A \tag{3}$$

where ρ is specific resistivity, L is the length, and R and A are the resistance and sectional area, respectively. The specific resistivity of the SPSed thin film was very similar to that of the film deposited using a target fabricated using the casting melting process.

Fig. 7 shows cross sectional TEM images of the sputtered thin film deposited on a Si substrate with a commercial and SPSed target. Both of the thin films were well deposited on the Si substrate and their thicknesses were about 500 nm. It was found that the crystallite sizes with columnar structures were about 32.6 ± 1.3 and 31.7 ± 1.5 nm in commercial and SPSed thin film, respectively. No defects such as voids and cracks were observed in the thin films.

Impurities analysis of the thin film having about 500 nm in thickness was carried out from the depth profiles of SIMS, and the results are shown in Fig. 8. The results show an almost similar profile aspect between the commercial and SPSed thin films. It was found that the intensities of impurity content of O and C in the layer of commercial thin film were higher than those of the SPSed layer. This could be attributed to the advantages of SPS having short sintering time and relatively low sintering temperature compared to the conventional sintering process, which could minimize the reaction between oxygen, carbon, and the target material during sintering. In the case of Al, Si, and Cu intensities, no difference is observed between the SPSed and commercial target thin films.

Conclusions

This study demonstrated that Al-1wt.%Si-0.5wt.%Cu

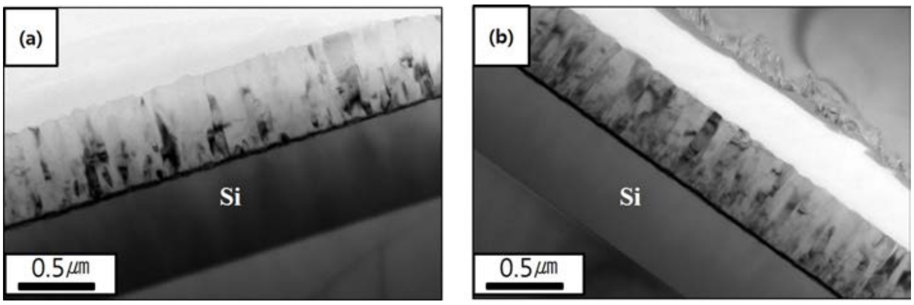

Fig. 7. Cross sectional TEM images of sputtered film. (a) Commercial and (b) SPS.

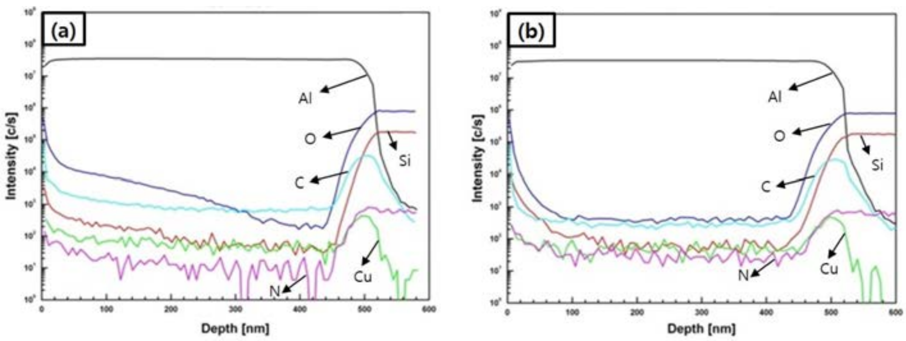

Fig. 8. SIMS depth profiles of sputtered films. (a) Commercial and (b) SPS.

sputtering target using high purity powder obtained from gas atomization process for semiconductor metallization applications can be successfully fabricated using spark plasma sintering method. From the study results, relatively low temperature and shorter processing times allow the sintering of Al-1wt.%Si-0.5wt.%Cu powder having full density and high purity with little grain growth. The properties of thin films deposited using the Al-1 wt%Si-0.5 wt.%Cu target fabricated from SPS were compared with those of the commercial target material prepared using the casting melting process. From these results, the properties of SPS thin films were almost similar to the commercial thin films. Therefore, a high quality SPSed sputtering target can be utilized as sputtering target materials for the device interconnection lines of a semiconductor.

Acknowledgments

This research was supported by an industrial source technology research project from the Ministry of Trade, Industry & Energy, Korea.

Reference

1. J. Sarkar, Sputtering targets and sputtered films for the microelectronic industry, ISBN No.978-0-8155-1593-7 (2014) 1-92.
2. J. Sarkar, Sputtering and thin film deposition, ISBN No.978-0-8155-1593-7 (2014) 93-170.
3. J. Sarkar, Sputtering target manufacturing, ISBN No.978-0-8155-1593-7 (2014) 197-289.
4. Y. Y. Chen, J. C. Hus, C. Y. Lee, W. P. Wang, J. Mater. Sci. 48 (2012) 1255-1230.
5. R. Bel Hadk Tahar, N. Bel Hadj Tahar, J. Am. Ceram. Soc. 88 (2005) 1725-1728.
6. S, Bader, E.M. Kalaugher, E. Arzt, Thin Solid Film 263 (1995) 75-184.
7. M.K. Mazumer, S. Yamamoto, H. Maeda, J. Komori. Y. Mashiko, Microelectr. Relat. 41 (2001) 1259-1264.
8. M. Zaborowski, P. Dumania, Microelectr. Eng. 50 (2000) 301-309.
9. B. Kaouache, P. Gerguad, O. Thomas, O. Bostorm, M. Legros, Microelectr. Eng. 70 (2003) 447-454.
10. S. Dietrich, M. Schneegans, M. Moske, K. Smawer, Thin films 275 (1996) 159-163.
11. H. K. Park, J. H. Ryu, H. J. Youn, J. M. Yang, I. H. Oh, Mater. Trans. 53 (2012) 1056-1061.
12. H.C. Kim, I.J. Shon, Z.A. Munir, J. Mater. Sci. 40 (2005) 2849-2854.
13. H.C. Kim, D.Y. Oh, I.J. Shon, Int. J. Ref. Met. Hard Mater. 22 (2004) 197-203.
14. H.C. Kim, H.K. Park, I.K. Jung, I.Y. Ko, I.J. Shon, Cermics Int. 34 (2008) 1419-1423.
15. M. Ranmall, powder metallurgy science, ISBN No. 1-878954-42-3, 100-116.
16. M. Bernard-Granger, C. Huizard, J. Acta Mater. 55 (2007) 3493-3504.